Journal of Applied Mechanics and Technical Physics, Vol. 36, No. 4, 1995

# STUDY OF THE BAUSCHINGER EFFECT UNDER DYNAMIC LOADING

S. A. Novikov, V. A. Pushkov, V. A. Sinitsyn, and P. A. Tsoi* UDC 539.389.2

To determine the load-carrying ability of members of structures under low-cycle loading, it is necessary to know the measure of the Bauschinger effect (BE). This effect, as a consequence of deformational anisotropy of materials, has been taken into account in some modern models of their mechanical behavior, in particular, in the model [1] based on the theory of small elastic–plastic deformations by Ilyushin and also in the thermoviscoplasticity model [2]. In the models the BE measure is among the basic scalar functions governing the shape and position of the center of an instant yield surface.

Typically, the quantity $\delta$ defined as

$$\delta = \begin{cases} \sigma'_{-\mathrm{y}}/\sigma_{+\mathrm{y}}, & \chi_\sigma = -1 \to +1, \\ \sigma'_{+\mathrm{y}}/\sigma_{-\mathrm{y}}, & \chi_\sigma = +1 \to -1 \end{cases}$$

is often used as the BE measure for tension–compression ($\chi_\sigma = -1 \to +1$) or compression–tension ($\chi_\sigma = +1 \to -1$) processes. Here $\sigma_{+\mathrm{y}}$, $\sigma_{-\mathrm{y}}$ are the "instant" yield limits under initial loading, which correspond to the residual strain $\varepsilon_t$ (Fig. 1); $\sigma'_{-\mathrm{y}}$, $\sigma'_{+\mathrm{y}}$ are the "instant" yield limits under succeeding alternate loading (they are determined for a given residual deformation tolerance); $\chi_\sigma$ is the Laudet parameter characterizing the type of stressed state.

It has been established that the BE for alloys and doped metals depends essentially on the previous elastic strain in a foregoing loading phase [1, 3]. Here $\delta$ decreases with increasing $\varepsilon_t$ and remains virtually constant at $\varepsilon_t \simeq 2$–4%. Generally, the BE measure is a function of deformation rate $\dot{\varepsilon}$, temperature $T$, as well as of $\varepsilon_t$ and $\chi_\sigma$: $\delta = \delta(\dot{\varepsilon}, T, \varepsilon_t, \chi_\sigma)$.

With no available data on BE, the calculations are based on the assumption that the classical Mazing principle is valid. For instance, $\sigma_{+\mathrm{y}} + |\sigma'_{-\mathrm{y}}| = 2\sigma^0_{+\mathrm{y}}$ ($\sigma^0_{+\mathrm{y}}$ is the yield limit at a starting tension) for tension–compression processes. However, the equality does not hold for the majority of materials and, therefore, the generalized Mazing principle is used: $\sigma_{+\mathrm{y}} + |\sigma'_{-\mathrm{y}}| = k_\sigma \sigma^0_{+\mathrm{y}}$, where $k_\sigma$ is determined as the BE measure $k_\sigma = (\sigma_{+\mathrm{y}} + |\sigma'_{-\mathrm{y}}|)/\sigma^0_{+\mathrm{y}} = (1+\delta)\sigma_{+\mathrm{y}}/\sigma^0_{+\mathrm{y}}$. It has been shown [1, 4, 5] that the Mazing principle, when compared with other known methods of construction of repeated strain diagrams by the initial one (for example, by the methods of [3, 6]) reflects the physical nature of repeated strain processes most fully.

Though the studies in the field were started as early as in the late XIXth century [7], the BE is still studied insufficiently and under static loading only. Meantime, alternate low-cycle loadings are predominantly of a dynamic nature. The difficulties in realization of the alternate dynamic loading of a specimen seem to be the main reason for the present state of the problem.

Apparently, the first successful attempt to experimentally determine the BE under dynamic loading was made in [8].

The technique for studying the dynamic BE in structural materials based on the method described in [8] and the first results obtained with steel St. 3 are discussed in this paper.

*Deceased.

Russian Institute of Experimental Physics, Arzamas-16 607200. Translated from Prikladnaya Mekhanika i Tekhnicheskaya Fizika, Vol. 36, No. 4, pp. 163–169, July–August, 1995. Original article submitted August 12, 1994.

 0021-8944/95/3604-0622 $12.50 

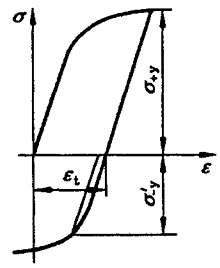


Fig. 1

**1. Theoretical Approach.** In [8], it is proposed that a three-step rod, in which the processes of propagation, reflection, and transformation of stress waves occur upon an impact of a pin on a step, be used in order to achieve dynamic low-cycle alternate loading.

According to the theory of propagation of stress elastic waves , a stress wave $\sigma_I(x - c_1 t)$ incident upon an interface between media with different acoustic stiffnesses $A_i\rho_i c_i$ $(i = 1, 2)$ is the sum of the passing $\sigma_y(x - c_2 t)$ and reflected $\sigma_R(x - c_1 t)$ wave.

Hence, the following equations are true:

$$\begin{gathered}\sigma_y/\sigma_I = 2A_1\rho_2 c_2/(A_1\rho_1 c_1 + A_2\rho_2 c_2),\\ \sigma_R/\sigma_I = (A_2\rho_2 c_2 - A_1\rho_1 c_1)/(A_1\rho_1 c_1 + A_2\rho_2 c_2),\end{gathered} \tag{1.1}$$

where $A_i, \rho_i, c_i$ $(i = 1, 2)$ are the cross-section area, density, and sound velocity, respectively, of the media 1 and 2 ($c_i = \sqrt{E_i/\rho_i}$, $E_i$ is the modulus of elasticity of the media).

Figure 2 shows the propagation and reflection of stress waves in the Lagrangian coordinates $(x, t)$ under the impact of a tubular pin on a small step $B$–$B$ at velocity $V_0$. Here $A_0, A_1, A_2, A_3$ are the cross-section areas of the pin and sections *1*–*3* of the rod, respectively. It is assumed that the tubular pin and sections *2* and *3* of the rod have equal lengths, and the impact of the pin on the section $B$–$B$ of the rod gives rise to rectangular stress pulses in sections *1* and *2*. Stress pulses emerging in the cross-section $D$–$D$ of section *1* in time are shown in Fig. 2 also. The passing and reflected stress waves generated at the section boundaries obey Eq. (1.1).

Let $\sigma_0, \sigma_1, \sigma_2$ be stress waves emerging in the pin and sections *1* and *2* of the rod, respectively, upon the impact. We will show that in section *1* the primary stress wave $\sigma_1$ is followed by alternate stress waves $\sigma_5$ and $\sigma_9$, which can be expressed in terms of $\sigma_1$.

From the continuity conditions for the force and mass velocity at the $B$–$B$ interface we obtain the expressions [8]

$$A_0\sigma_0 + A_1\sigma_1 = A_2\sigma_2, \quad V_0 - \sigma_0/\rho c = -\sigma_1/\rho c = \sigma_2/\rho c. \tag{1.2}$$

Here $\rho$ and $c$ are the density and sound velocity, respectively, in the pin and the rod (it is assumed that both are made of the same material).

Likewise, for the $C$–$C$ interface of sections *2* and *3*, the following equations hold:

$$A_2(\sigma_2 + \sigma_4) = A_3\sigma_3, \quad (\sigma_2 - \sigma_4)/\rho c = \sigma_3/\rho c, \tag{1.3}$$

where $\sigma_3$ and $\sigma_4$ are the passing and reflected stress waves emerging after incidence of the stress wave $\sigma_2$ upon the $C$–$C$ interface.

Amplitudes of $\sigma_0$, $\sigma_2$, $\sigma_3$, and $\sigma_4$ can be found from Eqs. (1.2) and (1.3) in terms of $V_0$, $A_0$, $A_1$, $A_2$, $A_3$, $\rho c$, and $\sigma_1$. Then $\sigma_1 = \rho c V_0 A_0/(A_0 + A_1 + A_2)$, and $\sigma_2, \sigma_3, \sigma_4$ may be expressed in terms of $\sigma_1$, $A_1$, $A_2$, and $A_3$.

With the help of (1.1)–(1.3) and similar equations describing the passage of the stress waves $\sigma_4$ and $\sigma_7$ through the $B$–$B$ interface (Fig. 1), after some transformations we shall get the equations for $\sigma_5$ and $\sigma_9$:

$$\sigma_5 = \lambda\sigma_1, \quad \sigma_9 = \mu\sigma_1. \tag{1.4}$$

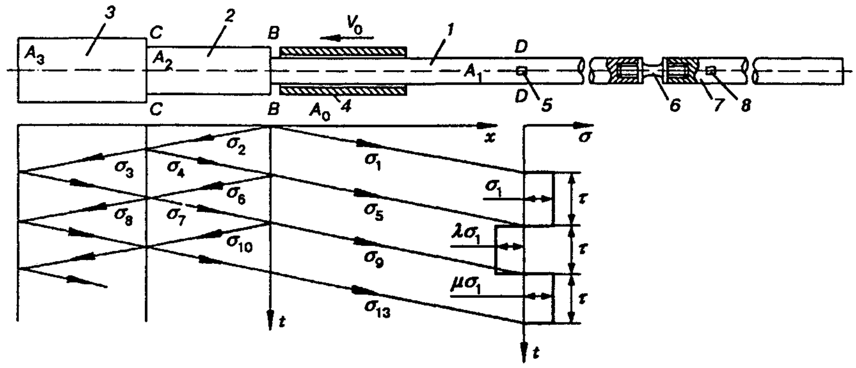


Fig. 2

Here

$$\lambda = 2(\beta - 1)/(\alpha + 1)(\beta + 1);$$

$$\mu = 2\,[4\beta(\alpha + 1) - (\alpha - 1)(\beta - 1)^2\,]/(\alpha + 1)^2(\beta + 1)^2;$$

$$\alpha = A_1/A_2; \quad \beta = A_2/A_3; \quad \alpha > 0; \quad \beta > 0.$$

Since $A_1 < A_2 < A_3$, it is apparent that $\lambda < 0$, $\mu > 0$.

Thus, the alternating stress waves $\sigma_1, \sigma_5, \sigma_9$ run to the right at section *1* of the rod.

Amplitudes of succeeding cyclic stress waves running to the right through the cross-section $D$–$D$ of the rod can be found in the same manner. If a test bar is placed at a certain distance from the step $B$–$B$, it is loaded with these alternating stress waves and undergoes cyclic elastoplastic deformation (Fig. 2).

The described technique for achieving alternate loading is the basis of the method we suggest to study the dynamic BE.

A layout similar to Kolskii's dynamic test design involving Hopkinson's split-bar [9] can be produced by fixing one end of the piece to be tested in a three-step rod (loading rod) and other in one-step rod (supporting rod).

The stress $\sigma(t)$ and strain $\varepsilon(t)$ of the specimen needed to plot $\sigma - \varepsilon$ diagrams are found by the Kolskii method [9] as follows:

$$\sigma = E\varepsilon_{\rm I}(t)A_1/A, \quad \varepsilon = (2c/l)\int_0^t [\varepsilon_{\rm I}(t) - \varepsilon_{\rm y}(t)]\,dt, \tag{1.5}$$

where $A$, $l$ are the cross-section area and the length of the working section of a specimen; $E$ and $c$ are the elasticity modulus and sound velocity in the rods, respectively; $\varepsilon_{\rm I}(t)$ is the elastic deformation in the incident stress wave initiated in the cross-section $D$–$D$; $\varepsilon_{\rm I}(t)$ is the elastic defromation in a stress wave passing toward the supporting rod.

The strain rate $\dot{\varepsilon} = d\varepsilon/dt$ is determined in terms of the strain law $\varepsilon = \varepsilon(t)$, i.e., from (1.5):

$$\dot{\varepsilon} = (2c/l)[\varepsilon_{\rm I}(t) - \varepsilon_{\rm y}(t)].$$

**2. Experimental Procedure.** The above theoretical approach was used to develop a test device for investigating the dynamic BE in materials. The basic unit of the device is similar to that shown in Fig. 2. A three-step loading rod with sections *1–3* of diameters $d = 12$, 22, and 45 mm, respectively, is made of steel 30HGSA. Supporting rod *7* (Fig. 2) 12 mm in diameter is also made of steel 30HGSA. Tubular pin *4* (steel 30HGSA, $d = 21 \times 16$ mm) is of the same length as sections *2* and *3* of the loading rod. In the experiments the pin was accelerated using explosive charge energy. Tension resistors *5* and *8* are used to record elastic deformation pulses $\varepsilon_{\rm I}(t)$ and $\varepsilon_{\rm y}(t)$, respectively, in the rods. The two ends of bar *6* of stay type with a working section $d = 5 \times 8$ mm in size are threaded to be fixed in the rods. To eliminate gaps between the bar end and

TABLE 1

| $\dot{\varepsilon}_t$, sec$^{-1}$ | $\varepsilon_t$, % | $\sigma^d_{+0.1}$ | $\sigma^d_{+y}$ | $\sigma^d_{-0.1}$ | $\delta^d$ |
|---|---|---|---|---|---|
| | | MPa | | | |
| 680 | 0.95 | 540 | 580 | 315 | 0.54 |
| 700 | 0.92 | 580 | 635 | 310 | 0,49 |
| 680 | 0.46 | 560 | 585 | 415 | 0.71 |
| 540 | 0.96 | 525 | 590 | 220 | 0,37 |
| 450 | 1.05 | 530 | 585 | 270 | 0.46 |
| 510 | 1.20 | 530 | 600 | 200 | 0.33 |
| 520 | 1.40 | 535 | 605 | 195 | 0.32 |
| 410 | 0.66 | 560 | 590 | 335 | 0.57 |

thread hollows, contact plates made of alumina alloy AMTs were used.

The test device was positioned at the center of the tube body and placed on a channel frame with an angle piece which supported the free end of step *3* of the loading rod.

Additionally, the device was equipped with a number of gadgets to prevent the construction and measuring lines from the undesirable effects of explosive loading.

In the experiments the pin was accelerated and struck a small shoulder of the loading rod. Then, a tension stress wave $\sigma_1$ ran to the right of the shoulder, and a compression stress wave $\sigma_2$ to the left (Fig. 2), the latter being transformed to a compression stress wave $\sigma_5 = \lambda\sigma_1$, which ran to the right of the shoulder. The process of dynamic tension-compression of the bar occurred. According to the above theoretical approach, the wave $\sigma_5$ is followed by alternating waves $\sigma_9, \sigma_{13}, \ldots$, giving rise to further cycles of tension and compression of the bar.

At a fixed velocity $\dot{\varepsilon}$ and temperature $T$, the residual strain $\varepsilon_t$ depends only on the duration $\tau$ of pulses $\sigma_1, \sigma_5, \ldots$ (Fig. 2). Therefore, the lengths of sections *2* and *3* of the loading rod and the pin should be varied in order to find the dependence $\delta = \delta(\varepsilon_t)$. With this aim, the device is equipped with interchangeable rods and pins of four standard sizes.

In order to find $\delta = \delta(\dot{\varepsilon})$ at $\varepsilon_t$ = const and $T$ = const, the strain velocity $\dot{\varepsilon}$ during the first tension phase is varied by changing the impact velocity $V_0$ through variations of the explosive charge weight. The strain velocity during the second compression phase can be controlled by varying the coefficient $\lambda$ [see Eq. (1.4)], i.e., by changing the ratios of the cross sections $A_1$, $A_2$, $A_3$ of the loading rod.

The device is equipped with a small cylindrical electric furnace in order to conduct high-temperature studies. The furnace is positioned near the specimen and is used to heat it and the butt-ends of both rods. Taking into account that the elastic properties of the rod material change on heating, the method is correctly applicable below 300°C. In the range 20–300°C the variation in the elasticity of steel 30HGSA is negligible.

**3. Results of First Experiments.** The dynamic BE in steel St. 3 was studied at an ambient temperature of 20°C (±5 °C). The observed strain velocity was 410–700 sec$^{-1}$ (speed of the pin 20–25 m/sec).

Figure 3 shows the typical strain pulses $\varepsilon_I(t)$ and $\varepsilon_y(t)$ for the first two loading phases in one of the experiments. The complete pulses of cyclic loading are sinusoids whose amplitudes are lowered by a factor of about 5 for $4 \cdot 10^{-3}$ sec.

Computer-aided processing of the results obtained was carried out using an ad-hoc procedure. A diagram of low-cycle tension–compression $\sigma - \varepsilon$ obtained at an average strain velocity of $\dot{\varepsilon}_p$ = 680 sec$^{-1}$ and residual deformation $\varepsilon_t = 0.95\%$ is shown in Fig. 4. Note that the fragments of the $\sigma - \varepsilon$ diagram related to the tension phase (above the abscissa) and the compression phase (below the abscissa) resulted from two independent runs; they were compiled under the assumption that the dynamic unloading of the specimen is linear and the unloading plot (dashed straight line) is parallel to the initial straight line of the stretching load.

The experimental results are summarized in Table 1, where $\dot{\varepsilon}_t = (\dot{\varepsilon}_{1t} + \dot{\varepsilon}_{2t})/2$ is the average velocity of plastic strain ($\dot{\varepsilon}_{1t}$ and $\dot{\varepsilon}_{2t}$ are the strain velocities in the plastic regions of the $\sigma - \varepsilon$ diagram in the phases

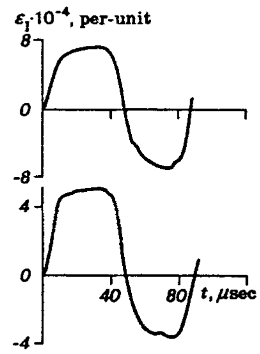


Fig. 3

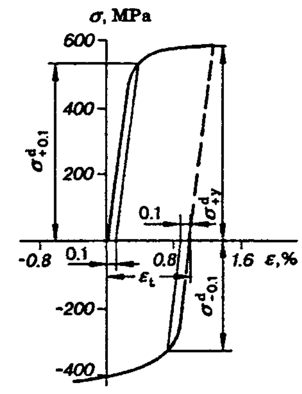


Fig. 4

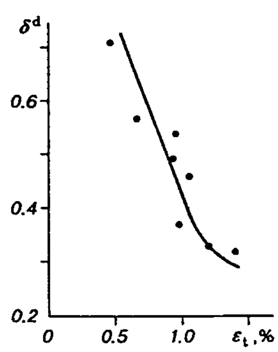


Fig. 5

of tension and compression, respectively; they differ by not more than 15%), $\varepsilon_t$ is the residual strain of the bar in the tension phase, $\sigma^d_{+0.1}$ is the dynamic yield point in the tension phase, $\sigma^d_{+y}$ is the "instantaneous" dynamic yield limit in tension, corresponding to the residual strain $\varepsilon_t$, $\sigma^d_{-0.1}$ is the modulus of "instantaneous" dynamic yield limit in the compression phase, corresponding to the residual strain $\varepsilon_t$, and $\delta^d = \sigma^d_{-0.1}/\sigma^d_{+y}$ is the measure of the dynamic BE.

Note that no dependence of $\delta^d$ on $\dot{\varepsilon}_t$ was found within the studied range of strain velocities. The results obtained for $\delta^d$ were not compared to the data on static loading because of the lack of such data for St. 3. The data available for this steel refer mainly to the low-cycle strengths of various structure members (e.g., [10]). A somewhat conventional comparison may be made with the BE reported in [11, 12] for various steels under static tension–compression at $\varepsilon_t = 0.2\%$. The BE in steels 20 and 25 (among the studied steels, they are closest to St. 3 in chemical composition) were found to be 39.4 and 29.6%, respectively. It should be noted that in [11] the BE measure is referred to as the change in the yield limit $\sigma_{-0.1}$ under tension following precompression to its initial value under the ordinary compression. In [12], it was found as the difference between the yield limits observed under tension and subsequent compression by using the equation

$$[(\sigma_{+0.1} - |\sigma_{-0.1}|)/\sigma_{+0.1}] \cdot 100\%. \tag{3.1}$$

Using the data obtained for steel St. 3 at $\varepsilon_t = 0.46\%$ under dynamic loading, the BE was calculated by Eq. (3.1) 25.9% (see the Table 1). The dependence $\delta^d = \delta^d(\varepsilon_t)$ was plotted (Fig. 5) using the data shown in Table 1. The data indicate that the BE in St. 3 is so significant that it should certainly be taken into account in the strength calculations. The above dependence generally decreases (the BE increases) as $\varepsilon_t$ increases, the BE change intensity being high at $\varepsilon_t \approx 1.1\%$ and decreasing rapidly at $\varepsilon_t \gtrsim 1.2\%$. Obviously, $\delta^d$ has to approach a limit value at $\varepsilon_t > 1.4\%$. This conclusion is consistent with the data reported in [1], according to which the BE [calculated by Eq. (3.1)] increases with an increase in steel prestrain, reaching a maximum at a prestrain of 1.5%.

To elucidate variations in the dynamic BE in steel St. 3 at $\varepsilon_t \lesssim 0.5\%$ and $\varepsilon_t > 1.4\%$, further studies are required. Here the behavior of $\delta^d$ at $\varepsilon_t > 1.4\%$ is of greater interest from the viewpoint of the determination of the limiting value of $\delta^d$ and manifestation of the BE under severe strains. Thus, pretension as high as 7.9% followed by repeated compression of steel 20 was shown [1] to produce a 71% decrease in the limit of proportionality.

Thus, a technique for investigating the dynamic BE in construction materials was developed on the basis of the method described in [8]. An explosive charge is used in the test device for low-cycle alternating loading during the investigations. The device allows one to conduct dynamic tension and compression of a test bar to produce various plastic strains at different strain velocities and temperatures. Initial data on the dynamic BE in steel St. 3 were obtained.

This work was supported by the Russian Foundation for Fundamental Research (Grant 93-01-16504).

## REFERENCES

1. V. V. Moskvitin, *Plasticity under Alternating Loads* [in Russian], Izd. Mosk. Univ., Moscow (1965).
2. Yu. G. Korotkikh and A. G. Ugodchikov, "The equation of thermoviscoplasticity with combined strengthening," in: *State Equations in Low-Cycle Loading* [in Russian], Nauka, Moscow (1981).
3. R. M. Shneiderovich, *Strength under Alternating Loading* [in Russian], Mashinostroenie, Moscow (1988).
4. A. P. Gusenkov and P. I. Kotov, *Long and Nonisothermal Low-Cycle Strength of Structure Members* [in Russian], Mashinostroenie, Moscow (1988).
5. H. A. Moreen, "Strain cycling effects in 1100 aluminum," *Trans. ASME, Ser. D, J. Basic. Eng.*, No. 1 (1990).
6. R. L. Wooley, "The Bauschinger effect in some face-centred and body-centred cubic metals," *Philos. Mag.*, **44**, 353 (1953).
7. I. Bauschinger, "Über die Veranderung der Elastizitatsgrenze und des Elastizitats Moduls verschiedener Metall," *Civil Ingenieur*, N. F. (1881).
8. K. Ogawa, "Impact-tension compression test by using a split-Hopkinson bar," *Exper. Mech.*, **24**, No. 2 (1984).
9. V. P. Muzychenko, S. I. Kashenko, and V. A. Gus'kov, "Application of the method of a split-Hopkinson bar to the investigation of dynamic properties of materials," *Zavod. Lab.*, No. 1 (1986).
10. A. P. Gusenkov and G. V. Moskvitin, *Low-Cycle Strength of Shell Structures* [in Russian], Nauka, Moscow (1989).
11. S. I. Ratner and Yu. S. Danilov, "Variations of proportionality and yield limit sunder repeated loading," *Zavod. Lab.*, No. 4 (1950).
12. K. Ya. Shults, "Some information on X-ray studies of the Baushinger effect," *Tr. Tallinn. Politekh. Inst.*, No. 172 (1960).